

10th CIRP Conference on Intelligent Computation in Manufacturing Engineering - CIRP ICME '16

Prediction of dressing in grinding operation via neural networks

Doriana M. D'Addona^a, Davide Matarazzo^{a,*}, Roberto Teti^a,
Paulo R. de Aguiar^b, Eduardo C. Bianchi^b, Arcangelo Fornaro^c

^aFraunhofer Joint Laboratory of Excellence on Advanced Production Technology (Fh-J_LEAPT Naples)

Dept. of Chemical, Materials and Industrial Production Engineering, University of Naples Federico II, Piazzale Tecchio 80, 80125 Naples, Italy

^bUniv. Estadual Paulista – UNESP – Faculty of Engineering, Department of Electrical Engineering, 17033-360, Bauru, SP, Brazil

^cAr.Ter. SrL, Via Padula 56/58, 80030 Castello di Cisterna (NA)

* Corresponding author. Tel.: +39 320 7173783. E-mail address: davide.matarazzo@unina.it.

Abstract

In order to obtain a modelling and prediction of tool wear in grinding operations, a Cognitive System has been employed to observe the dressing need and its trend. This paper aims to find a methodology to characterize the condition of the wheel during grinding operations and, by the use of cognitive paradigms, to understand the need of dressing. The Acoustic Emission signal from the grinding operation has been employed to characterize the wheel condition and, by the feature extraction of such signal, a cognitive system, based on Artificial Neural Networks, has been implemented.

© 2017 The Authors. Published by Elsevier B.V. This is an open access article under the CC BY-NC-ND license

(<http://creativecommons.org/licenses/by-nc-nd/4.0/>).

Peer-review under responsibility of the scientific committee of the 10th CIRP Conference on Intelligent Computation in Manufacturing Engineering

Keywords: Dressing; grinding; Acoustic emission signal; Artificial neural networks

1. Introduction

Grinding operations are abrasive processes which involve material removal. The material removal is carried out by the action of abrasive particles, positioned on a grinding wheel [1]. The grinding operation is one of the most common of all metalworking operations; even if abrasive processes are capable of high material removal rates, they are generally employed as a finishing operation.

Grinding processes are directly influenced by many factors, such as the workpiece, machine, grinding wheel and process settings. The monitoring and control of the process, not only allows to keep under control the process itself, but allows to improve the process performance and to avoid scraps and to reduce defects to a minimum possible to ensure high accuracy and quality [2].

The grinding wheel plays an important role in both the surface roughness and the material removal. The classification of the grinding wheel as “sharp” (with cutting capacity) or “dull” (with loss of cutting capacity) is fundamental to achieve the best performance of any abrasive operation [3, 4]. In order to understand the wheel conditions and to estimate

and approximate the wheel life cycle time, as accurate as possible, before the regeneration of the wheel through a dressing operation, the grinding operation itself was monitored. Through a sensor monitoring system, the Acoustic Emission (AE) signal was acquired and statistics derived from this signal. The combination of these statistics with the working parameters of the grinding operation will be employed to feed a cognitive decision making support system, such as an Artificial Neural Network (ANN) system, to determine the wheel condition at each grinding pass and to predict and estimate the dressing need.

Understanding and estimating the wheel life cycle before a dressing pass is fundamental to reduce the time and cost of the grinding operation itself, by minimizing the number of grinding passes without material removal and, furthermore, to avoid defects and to optimize the whole operation time.

Cognitive systems, such as Genetic Algorithms (GAs) and Artificial Neural Networks, are increasingly employed to optimize any kind of process and in the planning of any kind of engineering system [5 – 14]. ANNs are widely used in supporting the decision-making system of various manufacturing processes, such as lost wax casting processes,

to predict the tool-wear in milling and turning operations and to predict the dressing wear of grinding operations [8].

This research work focuses on a methodology for the prediction of the wheel wear and dressing need in cylindrical internal grinding operations. The aim of this study is, therefore, to supply a robust tool for the detection and prediction of the best time for the dressing operation, in order to minimize time for stops and to optimize the whole grinding operation.

2. Description of the grinding and dressing operation

The grinding operation were carried out at the Ar.Ter. SrL factory plant. The worked material was an AISI316; the performed operation was a cylindrical internal grinding, executed with the parameters indicated in Table 1, cooled with a water based coolant mixed to oil (4% oil, 96% water):

Table 1. Working parameters for each Test.

Parameters	Test 1	Test 2	Test 3
Material	AISI316	AISI316	AISI316
Feed rate [m/s]	0.00875	0.00875	0.00875
Speed of the spindle [rpm]	440	440	440
Speed of the piece [rpm]	40	40	40
Depth of cut per pass [mm]	0.03	0.03	0.05
Initial piece diameter [mm]	245.11	324.60	326.55
Required diameter	245.40	324.90	326.90
# of Passes	18	16	9

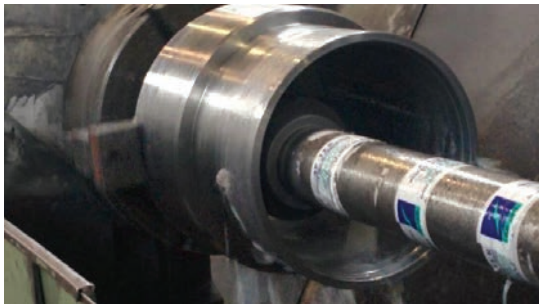


Fig. 1. Internal grinding operation at Ar.Ter. SrL.



Fig. 2. Dressing operation at Ar.Ter. SrL.

A parameter, which has been monitored and kept under control during the dressing operation of the wheel, was the overlap ratio [15]. The overlap ratio, Eq. 1, is a parameter which correlate the width of action of the dresser, b_d , which was assumed as a constant in each Test, and the dressing feed rate per wheel revolution, S_d , which was constant during each Test. From all of this, it comes that the overlap ratio, U_d , is constant for assumption

$$U_d = \frac{v_d}{r} \approx const. \quad (1)$$

The working piece was a CAGE16 component for Gas and Oil distribution pipes. Each piece was worked with the same conditions. The signal acquisition was performed on three test acquisition. The tests were carried out on a real production piece and, because of this, they had to be set with real production parameters, to avoid any scrap or defect. Basically, the test number three differs for the lowest number of passes, due to the deepest depth of cut set. The diameter of the working piece may also change, according to the production at Ar.Ter. SrL (Fig. 1). Starting from an initial diameter as the piece reached the working station for grinding, a material removal operation at the internal diameter was needed to set the piece at the data sheet specification. The abrasive grinding wheel, which was used for the material removal, was a Norton Silicon Carbide (SiC) 38A60LVS. The dressing passes (Fig. 2) were carried out by mean of a DIAVIK natural diamond at 1.5 carat weight; the diamond was mounted on a turned CM1 steel tool and the depth of cut was set at 0.03 mm. The feed rate of the wheel at 0.00875 m/s, turning at 440 rpm, without coolant. The wheel dimension was $d_{1,3} \times 50 \times 65$ mm, where $d_{1,3}$ was the diameter of the wheel measured for each of the three tests that varied from a maximum of 176 mm to a minimum value of 126 mm. The peripheral speed varied according to the wheel diameter used of each test and it oscillated from 4.05 m/s to 2.90 m/s.

3. Signal acquisition

The acoustic emission signal was acquired using the Montronix BV100™ broadband vibration sensor, provided with two channels to measure both the vibrations and the high frequency acoustic emission (AE) signals. The acoustic emission signal was acquired at 10 kHz. The analogue acoustic emission and sensor signals was then amplified by a Montronix TSVA4G amplifier. The specifications of the AE amplifier are reported in Table 2. The use of AE sensor signals has been widely employed to detect many phenomena in manufacturing processes, due to the working wide sensor bandwidth from 100 to 900 kHz [16, 17]. The AE sensor signals have as input a preamplifier with a high input impedance and low output impedance. Furthermore, a root mean square (RMS) converter, a gain selection unit, and filters are embedded in the preamplifier. In order to pass by this acquisition problem, the Montronix BV100™ was set to acquire RMS signals. The gain set for the acoustic emission RMS (AE_{RMS}) signals is equal to 10 to properly visualize the signals without exceeding the maximum threshold of 10 V imposed by the data acquisition (DAQ) board.

Table 2. Montronix TSVA4G specifications.

Parameter	Value
Gain Settings:	1, 2, 5, 10, 20, 40, 80, 200, 400, 800
Gain Error	±2%
Output Voltage	0 to 10 V
Power provided to Sensor	+ 15 VDC @ 4mA constant current
Amplifier Power Requirements	+15 VDC @ 80mA -15 VDC @ -60 mA
Temperature Range	0° to 60° C
Connectors	PG9 threaded fittings, sensor-specific
Weight	680 g



Fig. 4. Signal acquisition system.



Fig. 5. Montronix AE BV100 sensor.

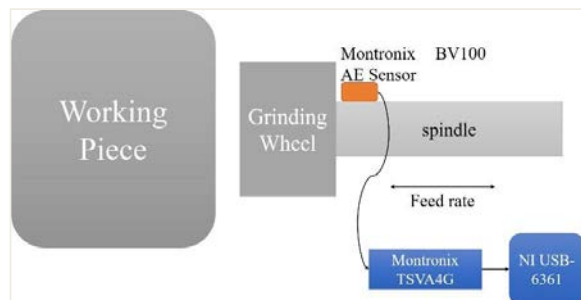


Fig. 6. Experimental setup and tests.

The time constant for RMS was set as short at 0.12 ms. The AE signal has been acquired as RMS signal. RMS is a technique used to rectify a RAW signal and convert it to an amplitude envelope, besides other significances; it is a measure of energy content in a given signal and, therefore, is widely used in monitoring systems. The rectification process converts all the numbers into positive values rather than positive and negative. The analogue signals from the AE_{RMS} sensors were digitalized by the National Instruments DAQ device NI USB-6361. The NI Signal Express 2014 software was used to acquire the data. Figures 4 - 6 illustrate the acquisition process and the experimental setup.

4. Data Processing and elaboration

The process consisted of a set of three tests of grinding operations. Each test counted a number of about 20 passes. As the operator detected that the effectiveness of the grinding lowers, a dressing operation was required. Each grinding/dressing pass was assigned a stored file, which was identified with the coded name "PASS m ", with $m = 001, \dots, n$.

For each pass the workpiece condition was monitored and measured, until the desired diameter and the planned material removal was reached. Figure 7 (a - c) shows the AE_{RMS} signals acquired during Test 1 and they refer to the TEST 1 - PASS002, TEST 1 - PASS012 and TEST 1 - PASS022. The Figures show the whole AE_{RMS} signal during the acquisition, which contains noise and tails.

In order to avoid the undesirable signal segments and thus to work on the signal itself during grinding, the AE_{RMS} signal needs to be cut and filtered. To identify the start and end of the actual signals, they were cut on the basis of thresholds fixed on the moving average (Figure 8, a - c) of AE signal for each pass. The filtering process was carried out by using a low-pass filter, with cutting frequency of 10 Hz.

In Figure 8 (a) it is important to notice that the signal sequence keeps low values of voltage and it has a low oscillation during the pass, while in Figure 8 (b) it can be noticed more oscillations and voltage values higher. This is precisely due to the fact that TEST 1 - PASS002 is the start of the processing, and it was performed after a dressing pass. While TEST 1 - PASS012 is right before the dressing operation. In Figure 8 (c), TEST 1 - PASS022, it can be noticed a high oscillation trend.

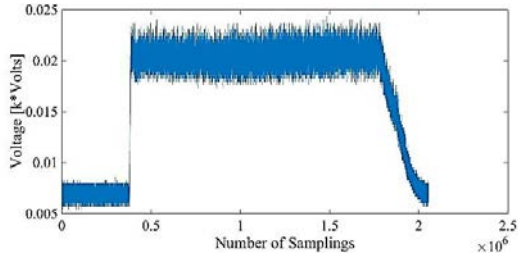
The AE_{RMS} signals were then segmented at the same start and end points for every pass, in order to obtain signals with equal duration and number of samplings (Figures 9 a - c).

5. Feature Extraction

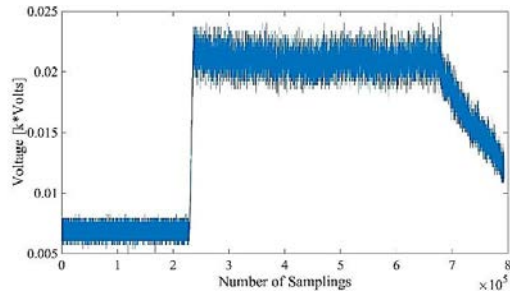
The relevant features from the signal extraction is critical to define the intrinsic characteristics of the signal itself, in order to then use the same for the supply of a cognitive system based on artificial neural networks. Features can be extracted from the AE_{RMS} sensor signals in the time domain. These features have been extracted and selected on the basis of their capability to describe the signal itself and are related to the process and the tool condition. In this case, the tool

condition is given by the need of dressing, according to the capability of the wheel to remove material. The most common signal features in the time domain, and those selected to feed the ANN decision making system, are the following [17 – 20]:

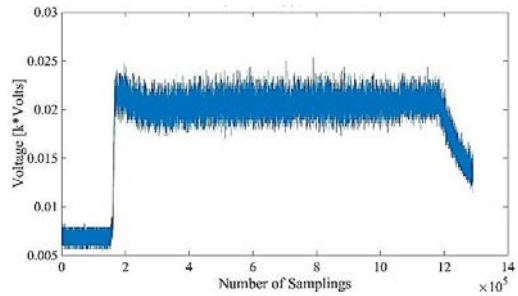
- Arithmetic features: mean and average value of the signal;
- Conventional statistical features: variance, kurtosis, skewness;
- Acoustic emission energy [21 -23].



(a)

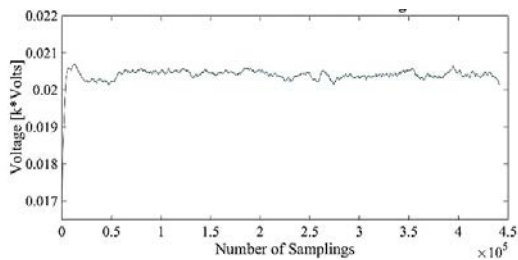


(b)

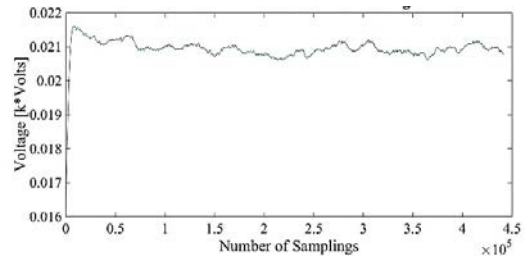


(c)

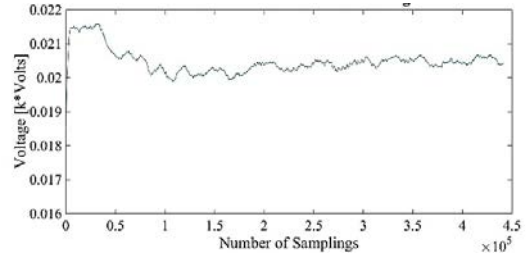
Fig. 7. (a) PASS002, (b) PASS012, (c) PASS022 AE signals.



(a)

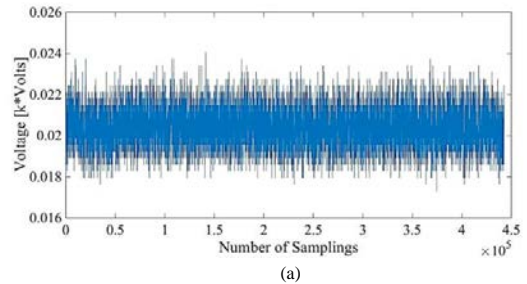


(b)

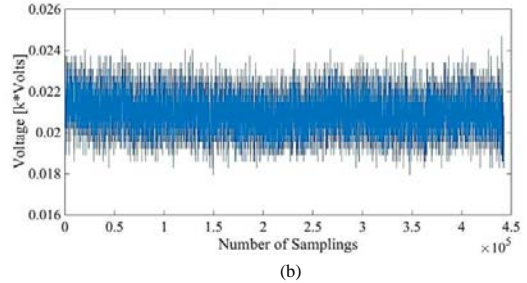


(c)

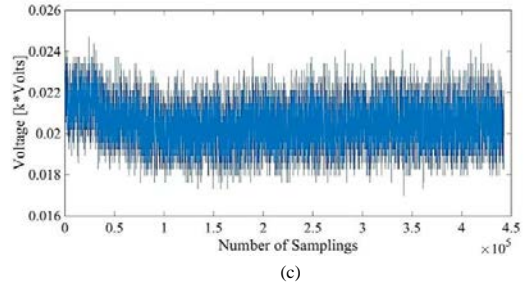
Fig. 8. (a) PASS002, (b) PASS012, (c) PASS022: Moving Average of the AE_{RMS} signals.



(a)



(b)



(c)

Fig. 9. (a) PASS002, (b) PASS012, (c) PASS022: Signal portion of the AE signals.

In particular, audible sound energy appears to be an effective tool that could adequately replace operator's experience based on knowledge. Audible sensing techniques have been widely investigated for grinding and dressing operations. The investigation on the relationship between tool condition and measurable signals for the detecting of the dressing need has been extensively studied. In particular, the use of AE signal allows to monitoring the tool condition from the AE feature extraction. AE signals differ from the vibration signals as they are not influenced by the environment noises without interfering with the process. In order to feed the ANN decision-making system, the aforementioned features have been combined with the working parameters of the grinding operation, such as the followings [24, 25]:

- Feed rate [m/s]
- Depth of cut [mm]
- Peripheral speed of the workpiece and of the wheel [m/s]
- Internal diameter [mm].

6. Cognitive system implementation

The foregoing features have been employed as the input of the ANN decision-making system, while the output has been identified in the need of dressing during the grinding operation. To associate the output with a wheel condition, a classification of the grinding wheel as "sharp" (with cutting capacity) or "dull" (with loss of cutting capacity) has been made. In particular, the condition "sharp" has been classified as output with the *code 0*, while the condition "dull" has been classified with the *code 1*.

The input matrix of the network is then composed by 43 rows, where 18 refers to the TEST 1, 16 to the TEST 2, 9 to the TEST 3. The matrix has by ten columns, which are representative of a machining parameter (feed rate, depth of cut, peripheral speed of the workpiece, peripheral speed of the wheel, amount of material removed) and of a feature extracted from the signal (average value of the signal, kurtosis, variance, skewness, acoustic emission energy). While for TEST 1 and 2 the machining parameters are quite the same, they are slightly changed for TEST 3, depending on the geometry of the workpiece, which was slightly different. The signal features have been extracted from the corresponding AE_{RMS} signals. The vector of the encoded output was created by associating each row of the matrix to the corresponding condition of the grinding wheel. In fact, has been assigned *0* when the grinding wheel was sharp and therefore able to remove material, and *1* for the dull grinding wheel, which was the last roughing grinding before the operation of dressing, when the grinding wheel was no longer able to remove material. It should be noticed that, as regards the TEST 3, it has been set to a depth of cut greater, so as to further urge the wheel itself, and this was most evident in the number of dressing operations, however, associated with a lower number of passes for the achievement of the desired diameter.

The cognitive system for the decision making on the wheel condition and the need of dressing has been implemented through two ANN models: the first one relies on the *cascaforwardnet* (CFN) MATLAB R2014b function, while

the second relies on the *newcf* (NCF) MATLAB R2014b function. Both the models work with Backpropagation Neural Networks (BP NN) and have been found particularly indicated in understanding functional relationships between inputs and given outputs.

The CFN function is a three-layer neural network, which creates a weighted connection from the input and every previous layer, which are connected to the following layers and also creates connections from the input to all three layers [2, 26, 27].

The CFN function has been trained according to the train-validation-testing (T-V-T) method: in order to find the optimal percentage for the training, validation and testing phase, an optimization based on the L_1 norm has been performed. Figures 10 and 11 show the optimal region in which the CFN function reaches the best performances, according to the given input and outputs. According to the Figures, the best region where to train the CFN function is the region highlighted in red, where the ANN reaches the lowest value of the norm L_1 , according to a given node number and a given training set dimension.

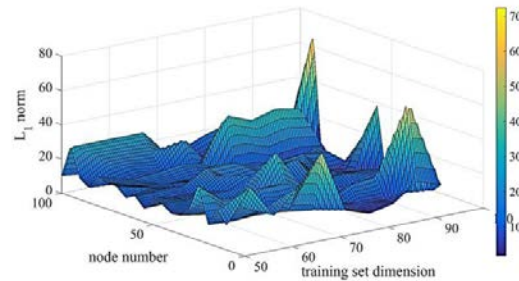


Fig. 10. 3D surface investigation on L_1 norm performances.

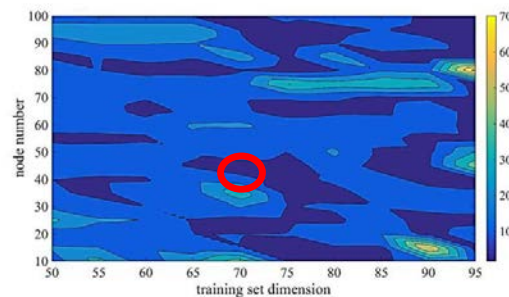


Fig. 11. 2D surface investigation on L_1 norm performances.

The second neural network model was based on the *newcf* function. While the CFN has been optimized on the basis of the T-V-T method, the NCF optimization has been carried out by the use of the *leave-k-out* (L-k-O) method. By setting $k=1$, this method creates a testing variable by leaving out the k -th row of the input matrix and of the output vector and it performs the training with the remaining $n-k$ rows [2, 26, 27]. The performance test is performed by comparing the ANN predicted output with the testing variable k . Figure 12 shows the L_1 norm optimization of the NCF function, according to the number of epochs and number of nodes.

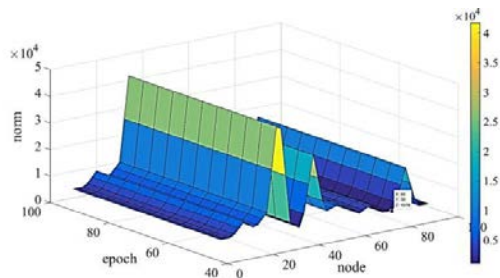


Fig. 12. 2D surface investigation on L_1 norm performances.

Table 3 shows the obtained results with both the CFN and NCF function. The number of nodes and the best setting for each ANN has been chosen according to the lowest value of norm L_1 . The configuration which scored best is the CFN with 90 nodes and a Training given by the 70% of the input matrix. With this configuration, the ANN has been capable to predict the 100% of the “sharp” and “dull” wheel given condition.

Table 3. ANN results and summary.

NET	nodes	method	% training	Number of errors	
				#	%
CFN	40	T-V-T	70 -15 - 15	4	9.30%
CFN	55	T-V-T	70 -15 - 15	3	6.98%
CFN	26	T-V-T	70 -15 - 15	2	4.65%
CFN	90	T-V-T	70 -15 - 15	0	0.00%
NCF	30	L-k-O	FULL - K	13	30.23%
NCF	60	L-k-O	FULL - K	11	25.58%
NCF	90	L-k-O	FULL - K	10	23.26%
NCF	55	L-k-O	FULL - K	11	25.58%

7. Conclusions

The artificial neural network models were developed to obtain a robust decision making system. The system could be employed in real time and can support the operator during grinding operation with a view to optimization and continuous improvement of the performance.

References

- [1] Groover, M.P., 1996, *Fundamentals of Modern Manufacturing: Materials, Processes and Systems*, Prentice-Hall International Ed.
- [2] D'Addona, D.M., Matarazzo, D., Aguiar, P.R., Bianchi, E.C., Martins, C.H.R., 2016, Neural Networks Tool Condition Monitoring in Single-point Dressing Operations, *Procedia CIRP*, Vol. 41, pp. 431-436.
- [3] Moia, D. F. G., Thomazella, I. H., Aguiar, P. R., Bianchi, E. C., Martins, C. H. R., Marchi, M., 2015, Tool condition monitoring of aluminum oxide grinding wheel in dressing operation using acoustic emission and neural networks, *Journal of the Brazilian Society of Mechanical Sciences and Engineering*, 37(2).
- [4] Martins, C.H.R., Aguiar P.R., Frech, A., Bianchi E.C., 2014, Tool Condition Monitoring of Single-Point Dresser Using Acoustic Emission and Neural Networks Models, *Instrumentation and Measurement*, 63/3, p. 667-679.
- [5] D'Addona, D.M., Teti R., 2013, Genetic Algorithm-based Optimization of Cutting Parameters in Turning Processes, *Procedia CIRP*, 7, pp. 323-328.
- [6] Gimelli, A., Muccillo, M., 2013, Optimization criteria for cogeneration systems: Multi-objective approach and application in an hospital facility, *Applied Energy*, Vol. 104, pp. 910-923.
- [7] Teti, R., D'Addona, D.M., 2003, Grinding Wheel Management through Neuro-Fuzzy Forecasting of Dressing Cycle Time, *CIRP Annals*, Vol. 52/1, pp. 407-410.
- [8] D'Addona DM, Matarazzo D, Di Foggia M, Caramiello C, Iannuzzi S, 2015, Inclusion Scraps Control in Aerospace Blades Production through Cognitive Paradigms, *Procedia CIRP*, 33, pp. 322-327.
- [9] Missori, S, Sili, A, Ucciardello N, Process parameters optimization of laser beam welded joints by neural network, *Materials and Manufacturing Processes*, Volume 23, Issue 2, Feb. 2008, pp. 169-174.
- [10] Costanza G, Tata ME, Ucciardello N, Superplasticity in PbSn60: Experimental and neural network implementation, *Computational Material Science*, Volume 37, Issue 3, Sept. 2006, pp. 226-233.
- [11] Ferretti S, Caputo D, Penza M, D'Addona DM, 2013, Monitoring systems for zero defect manufacturing, *Procedia CIRP*, 12, p. 258-263.
- [12] Di Foggia M, D'Addona DM, 2013, Identification of critical key parameters and their impact to zero-defect manufacturing in the investment casting process, *Procedia CIRP*, 12, p. 264-269.
- [13] D'Addona DM, Teti, R., 2011, Multi-agent tool management in the manufacturing of aircraft engines, *Proceedings of the Institution of Mechanical Engineers, Part B: Journal of Engineering Manufacture*, 225, Issue 1, p. 62-73.
- [14] D'Addona, D.M., Genna, S., Leone, C., Matarazzo, D., 2016, Prediction of Poly-methyl-methacrylate Laser Milling Process Characteristics Based on Neural Networks and Fuzzy Data, *Procedia CIRP*, Volume 41, Pages 981-986.
- [15] Hassui A., Diniz A.E., 2003, Correlating surface roughness and vibration on plunge cylindrical grinding of steel. *Int J Mach Tools Manuf* 43:855–862.
- [16] Teti R, Buonadonna P, 1999, Round Robin on AE Monitoring of Machining. *Annals of the CIRP*, 48(3), p. 47–69.
- [17] Sick, B., 2002, On-line and indirect tool wear monitoring in turning with artificial neural networks: A review of more than a decade of research. *Mechanical Systems and Signal Processing*, 16(4), 487-546.
- [18] Dong, J., Subrahmanyam, K., Wong, Y., Hong, G., Mohanty, A., 2006, Bayesian-inference-based neural networks for tool wear estimation. *International Journal of Advanced Manufacturing Technology*, 30(9-10), 797-807.
- [19] Ghosh, N., Ravi, Y., Patra, A., Mukhopadhyay, S., Paul, S., Mohanty, A., Chattopadhyay, A., 2007, Estimation of tool wear during CNC milling using neural network-based sensor fusion. *Mechanical Systems and Signal Processing*, 21(1), 466-479.
- [20] Scheffer, C., Heyns, P., 2001, Wear monitoring in turning operations using vibration and strain measurements. *Mechanical Systems and Signal Processing*, 15(6), 1185-1202.
- [21] Jemielniak, K., 2000, Some aspects of AE application in tool condition monitoring. *Ultrasonics*, 38(1), 604-608.
- [22] Teti, R., Jemielniak, K., O'Donnell, G., 2010, Advanced monitoring of machining operations. *CIRP Annals - Manufacturing Technology*, 59(2), 717–739.
- [23] Rubio, E., Teti, R., 2009, Cutting parameters analysis for the development of a milling process monitoring system based on audible energy sound. *Journal of Intelligent Manufacturing*, 20(1), 43-54.
- [24] D'Addona, D.M., Teti, R., 2006, CBN Grinding Wheel Inventory Sizing through Non-Shortsighted Flexible Tool Management Strategies, 2nd Int. Virt. Conf. on Intelligent Production Machines and Systems, pp. 217-221.
- [25] Caggiano, A., Roberto Teti, R., 2013, CBN Grinding Performance Improvement in Aircraft Engine Components Manufacture, *Procedia CIRP*, Vol. 9, pp. 109-114.
- [26] D'Addona, D.M., Ullah, A.M.M.S., Matarazzo, D., 2015, Tool-wear prediction and pattern-recognition using artificial neural network and DNA-based computing, *Journal Article*, 0956-5515, *Journal of Intelligent Manufacturing*, Springer US, 2015-10-13, pp. 1-17.
- [27] Matarazzo, D., D'Addona, D.M., Caramiello, C., Di Foggia, M., Teti, R., 2016, Cognitive Decision-making Systems for Scraps Control in Aerospace Turbine Blade Casting, *Procedia CIRP*, Vol. 41, pp. 466-471.